Steady-State and Dynamic Modeling of Commercial Slurry High-Density Polyethylene (HDPE) Processes

Neeraj P. Khare, Kevin C. Seavey, and Y. A. Liu*

Honeywell Center of Excellence in Computer-Aided Design, Department of Chemical Engineering, Virginia Polytechnic Institute and State University, Blacksburg, Virginia 24061

Sundaram Ramanathan, Simon Lingard, and Chau-Chyun Chen

Aspen Technology, Inc., 10 Canal Park, Cambridge, Massachusetts 02141

We present the development of both steady-state and dynamic models for a slurry HDPE process using fundamental chemical engineering principles and advanced software tools, Polymers Plus and Aspen Dynamics. The discussion includes thermodynamic properties, phase equilibrium, reaction kinetics, polymer properties, and other modeling issues. We characterize a Ziegler−Natta catalyst by assuming the existence of multiple catalyst site types and deconvoluting data from gel permeation chromatography to determine the most probable chain-length distributions and relative amounts of polymer produced at each site type. We validate the model using plant data from two large-scale commercial slurry HDPE processes. Significantly, the model contains a single set of kinetic and thermodynamic parameters that accurately predicts the polymer production rate, molecular weight, polydispersity index, and composition for several product grades. We illustrate the utility of the dynamic model by simulating a grade change. Finally, we propose a process retrofit that permits an increase in the HDPE production rate of up to 20% while maintaining the product quality.

1. Introduction

1.1. Slurry HDPE Process Technology. The slurry polymerization of HDPE is the oldest and most widely used method of production. Figure 1 provides a flowchart for a typical slurry HDPE process. Slurry processes utilize either continuous stirred-tank reactors (CSTRs), as in our case, or loop reactors.[1] The monomers, chain-transfer agent, solvent, and catalyst species enter the reactors for polymerization. The vaporization of the solvent removes a large portion of the highly exothermic heat of polymerization. The resulting slurry undergoes separation, removing unreacted monomer, solvent, and oligomeric species from the polymer. Solvent is separated from the oligomer and recycled to the reactor inlets, and the oligomer is processed and packaged. Meanwhile, the polymer undergoes mixing, pelletization, and packaging.

The reactor temperature remains below the polymer melting point. The polymer crystallizes upon formation, creating a slurry of solid particles in the solvent.[1] The introduction of a comonomer species (typically propylene, 1-butene, or 1-hexene) allows for the adjustment of the polymer properties, because of the short-chain branches resulting from the alkyl groups on the comonomer. Increasing the comonomer content decreases the crystallinity of the polymer product and increases the rate of ethylene polymerization.[2] An increase in the comonomer content also decreases the polymer density and melting point.[1]

The major advantages of a slurry process include mild operating conditions, high monomer conversion, ease of heat removal, and relative ease of processing. Its disadvantages include long residence times (1−2.5 h per reactor), and limited production rates of polymers that have relatively low densities (lower than 0.940 g/cm^3) because of resin swelling.[1]

The Ziegler−Natta catalyst system involves a primary catalyst and a cocatalyst. The primary catalyst is a transition-metal salt, with a metal from groups IV to VIII of the periodic table. The cocatalyst is a base-metal halide or alkyl, with a metal from groups I to III.[3] Our modeled process uses titanium tetrachloride ($TiCl_4$) as the catalyst and triethyl aluminum [$Al(C_2H_5)_3$] as the cocatalyst.

Ziegler−Natta catalysts produce polymers with broad molecular weight distributions because of the chemical properties of the catalyst. Two theories currently exist that explain this heterogeneous behavior.[2] The first is the existence of different site types within the catalyst, each with its own reactivity, caused by differences in the local chemical compositions of the active sites. The second is the presence of transport resistances that affect the rate at which monomer species travel to the active sites. However, under most polymerization conditions, the effect of different catalyst site types is the dominating factor.[4] We therefore incorporate this catalytic effect by kinetically modeling multiple catalyst site types. We discuss this approach in section 3.5.

1.2. Modeled Processes. We obtained process data for eight grades of HDPE produced in two large-scale slurry polymerization plants (144 000 and 240 000 tons/year). In this paper, we present modeling methodology and results of modeling these two commercial plants. We refer to these as plant A and plant B, respectively. Each plant houses two production trains. One train has a parallel reactor configuration, and the other train has two reactors connected in series or tandem. In the

* To whom correspondence should be addressed. Phone: (540) 231-7800. Fax: (540) 231-5022. E-mail: design@vt.edu.

10.1021/ie020451n CCC: $22.00
Published on Web 10/22/2002

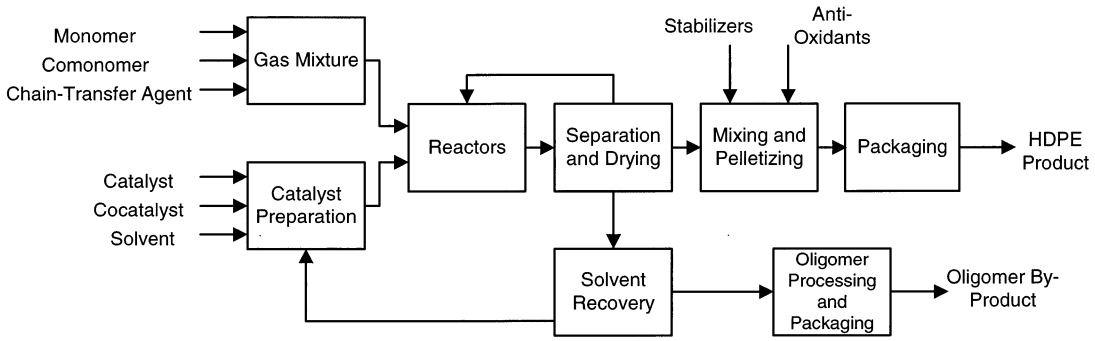

Figure 1. Flowchart of the slurry HDPE process.

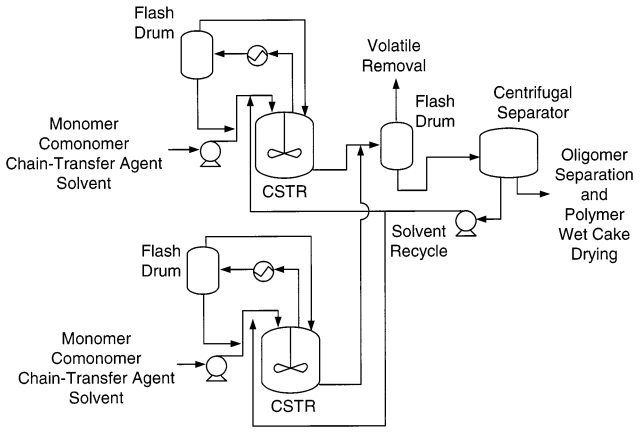

Figure 2. Process flow diagram for the parallel reactor configuration.

following sections, we provide more details about each configuration.

1.2.1. Parallel Reactor Configuration. Figure 2 shows the parallel arrangement, in which two continuous stirred-tank reactors (CSTRs) produce the HDPE. The comonomer for the parallel process is propylene. The slurry streams leaving the two reactors are combined and enter a flash unit for the removal of light hydrocarbons. The vapor streams leaving the reactors contain hexane, monomer, and light gases present in the system. These streams are cooled and flashed into vapor and liquid streams, which recycle to the monomer and solvent feed streams, respectively. The vaporization of hexane is the primary means for removal of the heat of polymerization. The polymer slurry leaving the flash unit enters a centrifugal separator that removes hexane from the polymer. This mother liquor returns to the reactor inlets, while the polymer stream travels to the processing and packaging phases of production.

1.2.2. Series Reactor Configuration. Figure 3 illustrates the series layout, where raw materials feed to the first CSTR and the slurry product is then pumped to the second CSTR, which also receives fresh monomer, catalyst, and solvent. The comonomer for the series process is 1-butene, and it enters only as a feed stream to the second reactor. The vapor outlet from each reactor undergoes cooling and recycles to the reactor inlet. The slurry stream leaving the second reactor enters a flash unit for removal of volatiles. The resulting stream enters a centrifugal separator, which removes and returns hexane to the reactor inlets.

Although the temperatures of the two reactors in the series configuration are the same, the hydrogen partial pressures are different, permitting the production of polymers with different average molecular weights in the two reactors. This results in a bimodal molecular weight distribution for the final polymer product. One can also vary the amount of comonomer fed to each reactor, providing a means of producing polymers with a variety of specific properties.[1]

1.3. Modeling Technology. Our modeling incorporates fundamental chemical engineering principles and advanced software tools for both steady-state and dynamic process simulation. We include mass and energy balances, thermophysical properties, phase equilibrium, polymerization kinetics, and reactor modeling.

We use both Polymers Plus and Aspen Dynamics to simulate the HDPE process. Polymers Plus applies process modeling technology to a wide variety of industrial polymerization processes. It considers the characterization of polymers and tracking of their structural properties throughout the flowsheet, phase equilibrium for polymer systems, polymerization kinetics, and reactor modeling.

Polymers Plus uses a segment-based approach for computing the physical properties of polymer species. By considering a polymer chain as a series of segments whose structures are well-defined, Polymers Plus can model the polymer properties that commonly vary with time in a synthesis process. This technique permits the modeling of properties such as molecular weight and copolymer composition and can account for the fact that most polymer products contain an ensemble of molecules having a distribution of chain lengths. It facilitates the use of group-contribution methods for the estimation of properties such as heat capacity, density, and melt- and glass-transition temperatures. One can also incorporate subroutines for user-defined correlations of polymer properties such as density and melt index.

Polymers Plus can interface with Aspen Dynamics to create dynamic models of polymer processes. We incorporate control schemes and track changes in polymer attributes with modifications of process variables such as reactor conditions or component feed rates. This integrated software package provides powerful modeling and predictive capabilities to the process design engineer.

2. Physical Properties

2.1. Introduction. Choosing appropriate property models for thermodynamic calculations can be a challenging endeavor. The phase behavior and thermophysical properties of polymer systems are generally much more complicated than those for conventional mixtures. One can describe the phase behavior of polymer systems by using activity-coefficient models and equations of state. The latter typically give pressure as

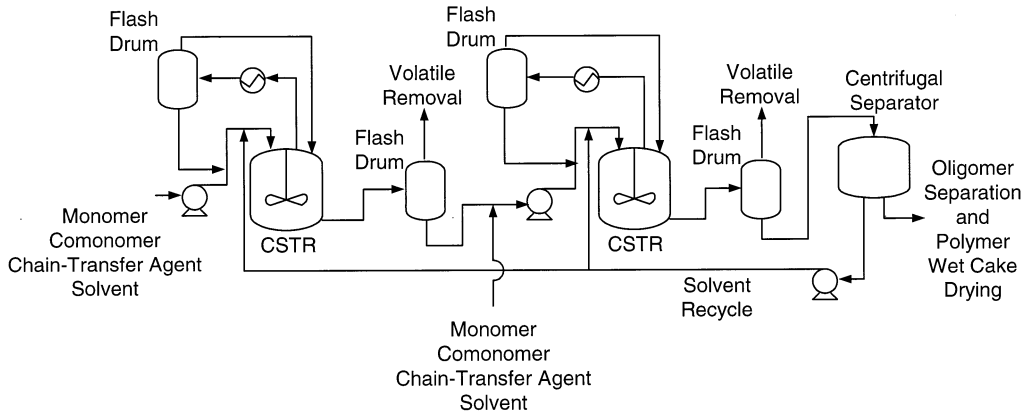

Figure 3. Process flow diagram for the series reactor configuration.

Table 1. Unit Operations for Which We Use the Sanchez−Lacombe and the Chao−Seader Property Methods

polymer-containing units (Sanchez−Lacombe method)	nonpolymer units (Chao−Seader method)
polymer reactors	raw-feed pumps
polymer devolatilizers (flash units)	overhead compressors
polymer recycle pumps	overhead flash units

a function of temperature, molar volume, and composition, while the former provide a correction to the ideal-solution assumption of Raoult's law.[5]

Because polymer equations of state do not normally perform as well as simple cubic equations of state for small components,[5] we use different property methods for the units and streams that contain polymer and those that do not. In the HDPE process, the polymer is present in the reactors and the subsequent separation units. The vapor recycle contains only monomer, solvent, and other small-molecule components, because the polymer is nonvolatile. We use the Sanchez−Lacombe equation of state for the polymer-containing sections of the plant and the Chao−Seader method for the nonpolymer areas. Table 1 lists the portions of the process model for which we use the Sanchez−Lacombe and Chao−Seader methods. We describe these methods next.

2.2. Sanchez−Lacombe Equation of State for Polymer Systems. We use an equation of state (EOS) developed by Sanchez and Lacombe[6−8] for the polymer-containing portions of the flowsheet. It is based on lattice theory, which states that fluids are mixtures of molecules and holes that are confined to sites in a lattice. The Sanchez−Lacombe EOS provides accurate predictions of the phase behavior and thermodynamic properties of the specific components in our system. It is valid for polymer species as well as conventional components. These predictions include molar volume; fugacity coefficients; heat capacities; and departures for enthalpy, entropy, and Gibbs free energy. The model is given by

$$\bar{\rho}^2 + \bar{P} + \bar{T}\left[\ln(1-\bar{\rho}) + \left(1 - \frac{1}{r}\right)\bar{\rho}\right] = 0 \qquad (1)$$

where $\bar{\rho}$, $\bar{P}$, and $\bar{T}$ are the reduced density, pressure, and temperature, respectively. These quantities relate to the density, pressure, and temperature via

$$\bar{\rho} = \frac{\rho}{\rho^*}, \quad \bar{P} = \frac{P}{P^*}, \quad \bar{T} = \frac{T}{T^*} \qquad (2)$$

where ρ^*, P^*, and T^* are scale factors that completely characterize each pure fluid. We typically determine values for these parameters by regressing experimental data for each species (usually, vapor-pressure data for conventional components and liquid-volume data for polymer species). Alternatively, we can use values published in the open literature, provided that the data used to obtain the parameter values were measured at or near the conditions of the modeled process. The Sanchez−Lacombe EOS also has two binary interaction parameters that one can determine by regressing binary phase data for the components of interest. Refer to sections 2.4 and 2.5 for the regressed parameter values and data sources we used.

2.3. Chao−Seader, Scatchard−Hildebrand, and Redlich−Kwong Models for Conventional Species. The Chao−Seader correlation provides excellent predictions of the reference-state fugacity coefficients for pure liquid hydrocarbons under our system conditions.[9] Its form is

$$\ln(\phi_i^{\mathrm{liq}}) = \ln(\nu_i^{(0)}) + \omega_i \ln(\nu_i^{(1)}) \qquad (3)$$

where $\nu_i^{(0)}$ and $\nu_i^{(1)}$ are functions of the system temperature and pressure and the critical temperature and pressure for component i and ω_i is the acentric factor for species i. The Chao−Seader method uses the Redlich−Kwong EOS for vapor-phase fugacities and the Scatchard−Hildebrand model for liquid activity coefficients.[10]

2.4. Pure-Component Properties. Table 2 lists the primary chemical species that exist in the slurry HDPE process. Impurities can be incorporated if their concentrations are significant. These might include hydrocarbons such as methane and ethane.

The component list includes segments for the monomer species. As described in section 1.3, Polymers Plus considers polymer species using a segment-based approach, where the macromolecules consist of chains containing segment versions of each monomer species. The polymerization reactions are written in terms of these segments as well.

A comprehensive model for the slurry HDPE process must provide an accurate description of the density, saturation pressure, heat capacity, and heat of vaporization for each species. This is especially important in the reactor because the kinetics calculations depend on accurate phase concentrations, and the heat of polymerization is primarily removed through the vaporization of the solvent, hexane.

Table 2. Components Used in the Slurry HDPE Process Model

species	function
titanium tetrachloride	catalyst
triethyl aluminum	cocatalyst
ethylene	monomer
ethylene segment	monomer segment
propylene	comonomer
propylene segment	comonomer segment
1-butene	comonomer
1-butene segment	comonomer segment
high-density polyethylene	polymer
oligomer	wax byproduct
hydrogen	chain-transfer agent
n-hexane	solvent
nitrogen	purge gas
methane	impurity
ethane	byproduct
propane	impurity
n-butane	impurity

Table 3. Pure-Component Parameters for the Sanchez−Lacombe EOS[a]

component	T^* (K)	P^* (bar)	ρ^* (kg/m^3)
catalyst	924.87	4000	866.97
cocatalyst	924.87	4000	866.97
hexane	483.13	2900	786
ethylene segment	663.15	4000	896.6
propylene segment	724.3	2800	938.87
1-butene segment	924.87	4000	866.97
ethylene	333	2400	631
propylene	360.43	3100	670.83
1-butene	396.62	2900	671.5
hydrogen	45.89	1000	142.66
nitrogen	140.77	1786.17	922.5
methane	224	2482	500
ethane	315	3273	640
propane	354.33	2800	615.91
butane	412.78	3257.9	755.68

[a] T^*, P^*, and ρ^* are the characteristic temperature, pressure, and density, respectively.

2.4.1. Sanchez−Lacombe Pure-Component Parameters. Table 3 provides pure-component parameters for the Sanchez−Lacombe EOS for relevant species. Note that, in Polymers Plus, one must enter the polymer unary parameters for the individual segments that comprise it. The density and heat-capacity data for polyethylene, polypropylene, and poly(1-butene) must be regressed and the resulting parameters used for each respective segment species. We choose parameters for the catalyst and cocatalyst such that they remain in the liquid phase.

Figure 4 compares model predictions with experimental data for the hexane saturation pressure. Figures 5−7 compare model predictions with experimental data for the densities of hexane, hydrogen, and ethylene, respectively. Figure 8 compares model predictions with data for the heat of vaporization of hexane. Both the Sanchez−Lacombe and Chao−Seader methods accurately describe these properties.

2.4.2. Heat Capacity. One can regress heat-capacity data for pure species to determine parameters for the ideal-gas heat capacity model used in enthalpy predictions

$$C_p^{ig} = C_1 + C_2 T \tag{4}$$

Table 4 gives the parameters for the major species in the slurry HDPE process.

Figures 9−11 compare model predictions with experimental data for the heat capacities of hexane, HDPE, and ethylene, respectively. Note that the EOS predictions tend to be less accurate near the critical region, producing small deviations at higher temperatures and pressures.

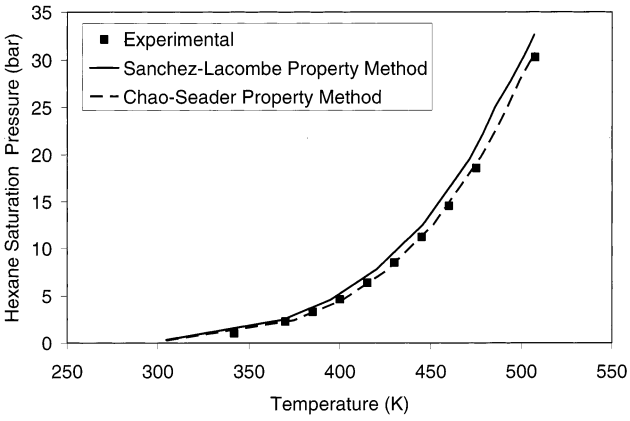

Figure 4. Saturation pressure of hexane.[11]

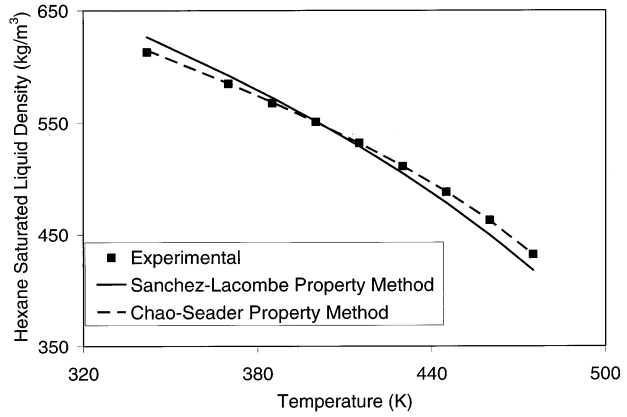

Figure 5. Saturated liquid density of hexane.[11]

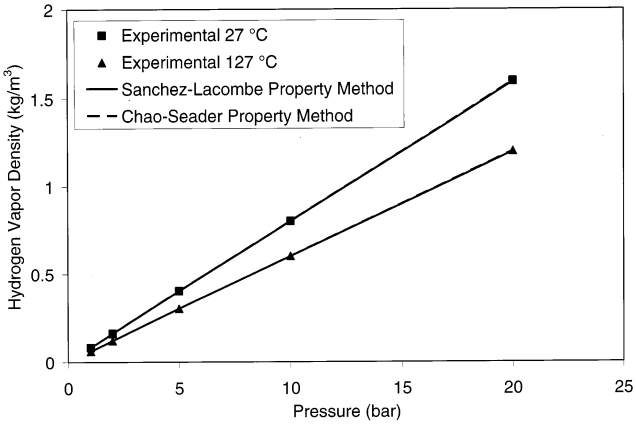

Figure 6. Density of hydrogen vapor.[11] The predictions of the two property methods are almost identical.

2.5. Mixture Properties. The vapor−liquid equilibrium in the slurry polymerization process is important because the solubilities of the monomer, comonomer, and hydrogen in the hexane directly affect the rates of reaction and the resulting polymer properties.

Tables 5 and 6 give values for each of the binary interaction parameters used in the Sanchez−Lacombe model. Unlike the case for the unary parameters, we use the HDPE species when specifying binary interaction parameters in Polymers Plus.

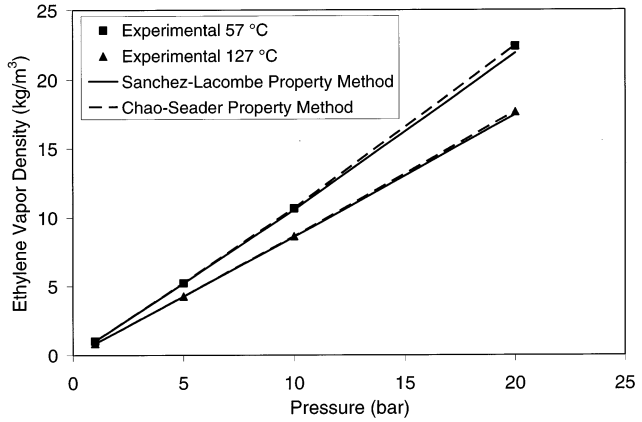

Figure 7. Density of ethylene vapor.[12]

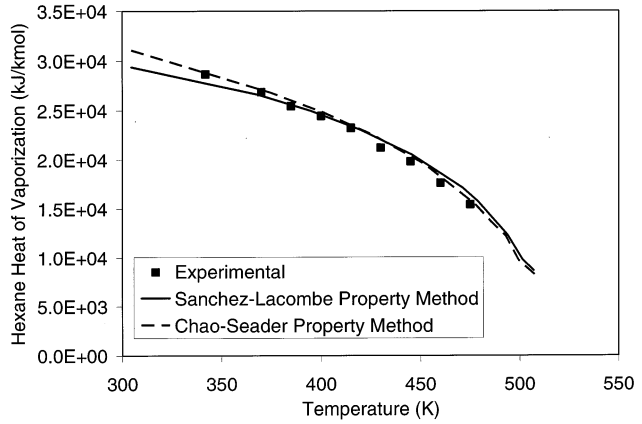

Figure 8. Heat of vaporization of hexane.[11]

Table 4. Parameters for the Ideal-Gas Heat Capacity (Eq 4)[a]

component	C_1	C_2
HDPE (R-C2H4)	3.51×10^4	68.22
HDPE (R-C3H6)	4.3205×10^4	133.58
HDPE (R-C4H8)	8.2932×10^4	115.29
hexane	1.6321×10^4	431.71
ethylene	2.3194×10^4	78.6581
propylene	1.0638×10^4	178.06
1-butene	4.6593×10^4	154.94
hydrogen	2.8332×10^4	1.96

[a] Values were determined by regressing pure-component data. Units for heat capacity are J/kmol·K.

Figure 12 compares model predictions with experimental data for the solubility of hydrogen in hexane. Hydrogen approaches the supercritical state under the conditions used in the HDPE process. Because the Sanchez−Lacombe EOS generally tends to overpredict the critical point, we do not use data near the critical region when determining pure-component parameters. For this reason, as well as the importance of the solubility prediction of hydrogen in the hexane solvent, we used the solubility data in Figure 12 to regress pure-component parameters for hydrogen.

2.6. Polymer Properties. 2.6.1. Heat of Polymerization. The heat of ethylene polymerization is the difference between the enthalpy of ethylene and the enthalpy, per segment, of the polymer under the same conditions. The reaction is[15]

$$C_2H_{4(g)} \rightarrow \frac{1}{n}(C_2H_4)_{n(\text{amorphous})}$$

$$\Delta H = -24.3 \text{ kcal/mol} \quad (5)$$

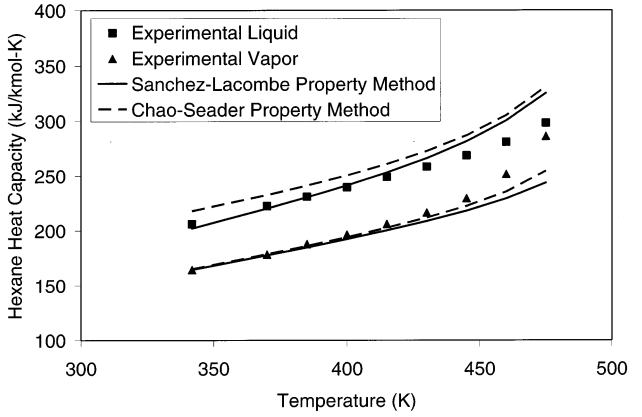

Figure 9. Heat capacity of liquid and vapor hexane.[11]

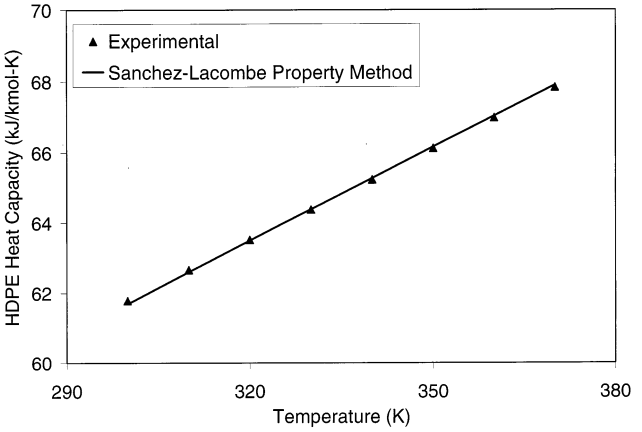

Figure 10. Heat capacity of HDPE.[13]

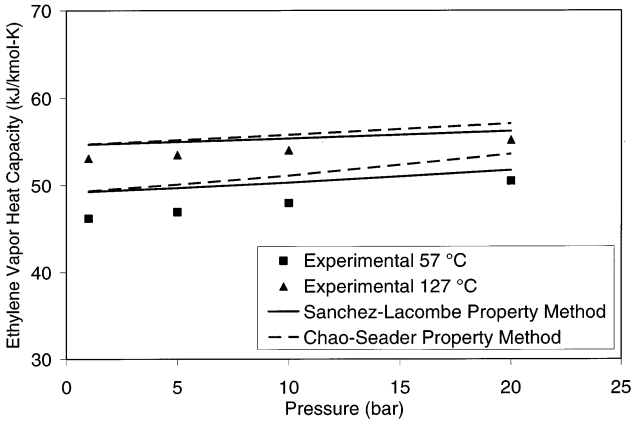

Figure 11. Heat capacity of ethylene vapor.[12]

Table 5. Values for Binary Interaction Parameters η_{ij} for the Sanchez−Lacombe EOS

	component j		
component i	ethylene	HDPE	hexane
hydrogen	−0.0867	−	0.100 705
ethylene	−	−0.1093	0.1476
1-butene	−	−	−
hexane	0.1476	−	−
propylene	−	−	0.14

where ΔH is the heat of ethylene polymerization. The difference between the enthalpies of ethylene and HDPE under the reactor conditions represents the heat of polymerization in the model. These enthalpies are computed using the Sanchez−Lacombe EOS. Table 7 gives model predictions for the heat of polymerization

Table 6. Values for Binary Interaction Parameters k_{ij} for the Sanchez–Lacombe EOS

	component *j*	
component *i*	hexane	HDPE
ethylene	0.0248	–
hexane	–	−0.14
methane	0.019 51	–
ethane	0.008 53	–
propylene	0.024 73	−0.14
hydrogen	0.100 705	–
butane	−0.002 286	–

Table 7. Computation of the Heat of Ethylene Polymerization Using the Sanchez–Lacombe EOS[a]

T (°C)	*P* (bar)	$H_{ethylene}$ (kcal/mol)	H_{HDPE} (kcal/mol)	ΔH_f (kcal/mol)
70	5	12.2	−12.7	−24.9
75	5	12.2	−12.6	−24.8
80	5	12.3	−12.5	−24.8
85	5	12.3	−12.4	−24.7
70	6	12.2	−12.7	−24.9
75	6	12.2	−12.6	−24.8
80	6	12.3	−12.5	−24.8
85	6	12.3	−12.4	−24.7

[a] Results compare favorably with the literature value given in eq 5.

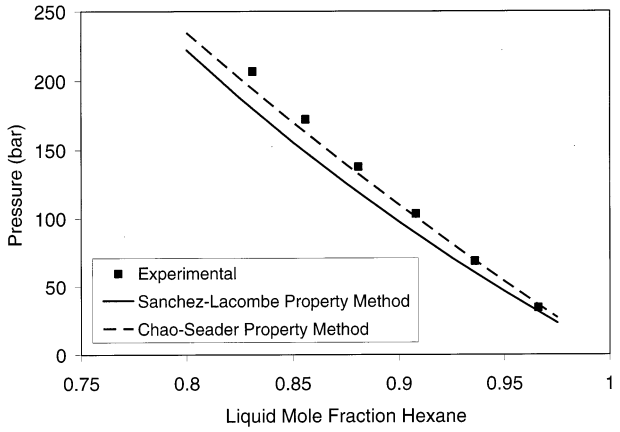

Figure 12. Solubility of hydrogen in hexane.[14]

for representative reactor conditions. These values compare favorably with the literature value given in eq 5.

2.6.2. Molecular Weight from Method of Moments. To model a polymer reactor rigorously, one would need individual rate expressions for polymer molecules of every chain length. Because polymers commonly contain distributions of chains consisting of up to hundreds of thousands of segments, this would lead to an impractical number of model equations. A useful technique for tracking the leading moments of the chain-length distribution of HDPE is the method of moments.[16] The moments are sums of polymer concentrations weighted by chain length. The moment expression for live polymer chains is

$$\mu_i = \sum_{n=1}^{\infty} n^i [P_n] \tag{6}$$

where μ_i is the ith moment for live chains and $[P_n]$ is the concentration of polymer chains containing

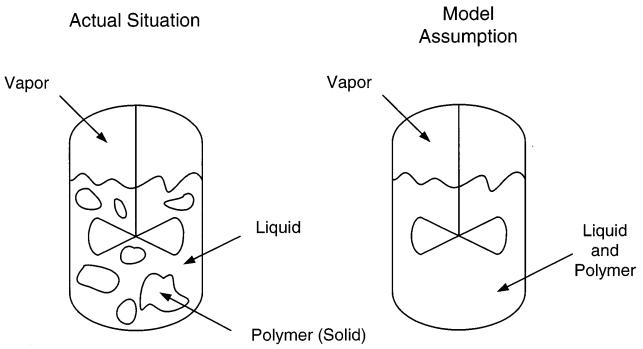

Figure 13. Comparison of the actual phase behavior in the reactor with the modeling assumption. The actual situation has vapor and liquid phases, with solid polymer dispersed in the liquid phase. Our system considers the polymer as solubilized in the liquid phase.

Table 8. Representative Species and Mass Fractions Used for Simulating the Phase Separation in a Slurry HDPE Reactor

component	mass fraction
ethylene	0.25
propylene	0.02
hexane	0.653
hydrogen	0.007
HDPE	0.07

n segments. The expression for bulk (live plus dead) chains is

$$\lambda_i = \sum_{n=1}^{\infty} n^i ([P_n] + [D_n]) \tag{7}$$

where $[D_n]$ is the concentration of dead (inactive) polymer chains. The rate expressions involving polymer chains are summed over all *n*, yielding a small number of closed expressions that are functions of the moments.

Typically, the zeroth, first, and second moments are sufficient for the computation of common polymer properties. Among them is the number-average molecular weight (M_n)

$$M_n = \frac{\lambda_1}{\lambda_0} \tag{8}$$

The weight-average molecular weight (M_w) is

$$M_w = \frac{\lambda_2}{\lambda_1} \tag{9}$$

The polydispersity index (PDI) is

$$\mathrm{PDI} = \frac{M_w}{M_n} = \frac{\lambda_2 \lambda_0}{\lambda_1^2} \tag{10}$$

Polymers Plus implements the method of moments approach in tracking polymerization kinetics and polymer properties.

2.7. Reactor Phase Equilibrium. As mentioned previously, the polymer forms a crystalline solid within the liquid phase upon formation. Solid polymer is generally considered to be inert and not to participate in phase equilibrium.[5] A rigorous approach would consider only the solubilities of gases that can dissolve in the solid polymer. However, most commercial process simulators do not have reactor models that permit the

Table 9. Comparison of the Liquid Compositions for Cases where the HDPE Has Its Own Liquid Phase (VLLE) and where It Is Dissolved in the Diluent (VLE)

	VLLE case			VLE case
species	liquid 1 (kg/h)	liquid 2 (kg/h)	total liquid (kg/h)	liquid (kg/h)
hexane	350.805 606 1	$9.815\ 07 \times 10^{-5}$	350.8057	367.9578
ethylene	5.520 240 829	0.351 363 342	5.871 604	5.466 046
propylene	1.248 687 94	$6.896\ 22 \times 10^{-5}$	1.248 757	1.495 278
hydrogen	0.007 724 188	0.000 382 869	0.008 107	0.014 171
HDPE	$1.200\ 71 \times 10^{-32}$	69.995 868 21	69.995 87	70

Table 10. Comparison of the Vapor Compositions for the VLE and VLLE Cases

	vapor mole fraction	
species	VLE case	VLLE case
hexane	0.207 643 2	0.217 584 7
ethylene	0.547 203 48	0.539 793 44
propylene	0.027 605 84	0.027 725 36
hydrogen	0.217 547 48	0.214 896 5

existence of distinct species that are thermodynamically inert. Alternatively, one can model the polymer as being dissolved in the liquid phase. Figure 13 compares these physically different situations. In the remainder of this section, we demonstrate that we can make this assumption without undermining the robustness of the reactor model.

We justify our simplification by comparing two approaches for modeling the slurry system. The first option is to treat the polymer as residing in a separate liquid phase (vapor−liquid−liquid equilibrium, VLLE), and in the second option, the polymer is treated as being dissolved in the solvent (vapor−liquid equilibrium, VLE). We model results for a flash vessel that simulates the phase separation for a mixture of components of mass fractions and conditions that are representative of an industrial slurry HDPE reactor. Table 8 gives the species and mass fractions that we use. For the case where HDPE is absent, we normalize the mass fractions of the remaining species to unity. We flash the mixture at 75 °C and 4 bar.

For the two-liquid case, we choose $k_{ij} = 0.5$ and $\eta_{ij} = 0$ for all polymer/conventional-component pairs to force the polymer into a separate liquid phase. Table 9 shows the resulting amounts of species in each liquid phase. The light components do not appreciably dissolve in the polymer phase. We also see that the differences in the total amounts of each species in the liquid phase for each case are relatively small.

Table 10 compares the vapor-phase predictions for each case. The vapor compositions are approximately the same. Because we use the same pressure in each case, these vapor fractions also represent the relative magnitudes of partial pressures of components in the mixtures.

In the VLLE situation, the reacting phase is the second liquid phase, and in our VLE simplification, it is the single liquid phase. Although the compositions of the reacting phases for these two approaches are different, the results are satisfactory. We can reasonably model the slurry HDPE process by considering the polymer as dissolved in the liquid phase (VLE) without compromising the predicted phase behavior of the major components.

3. Polymerization Kinetics

3.1. Introduction. The reactions and kinetics of Ziegler−Natta polymerization have been studied extensively for different catalyst systems and processes.[2,16−19] Further, it is generally accepted that Ziegler−Natta catalysts produce polymers with wide molecular weight distributions (MWD) because of the multisite nature of the catalyst. It is believed that there are several site types on the catalyst, each with its own reactivity. The composite polymer, defined as the sum of the polymer made from all of the catalyst sites, has a broad MWD even though the polymer made by each site type has a narrow (most probable) MWD.

In this work, we develop a multisite kinetic model for the slurry HDPE process. We select a subset of the Ziegler−Natta polymerization reactions that allows the model to describe the observed kinetic phenomena and match the production rate, melt index (MI), and density targets for several grades. Sections 3.2 and 3.3 describe the reactions for homopolymerization and copolymerization kinetics, respectively. We include additional reactions, described in section 3.4, to account for the production of wax (low-molecular-weight polymer species) that dissolves in the hexane diluent.

As there are many reactions and kinetic parameters, we develop a detailed methodology to fit the kinetic parameters to data for several grades from both the parallel and series modes of operation. The methodology, described in section 3.5, involves a three-step process to simplify the task of fitting the kinetic parameters. In the first step, we develop a single-site kinetic model and fit the rate constants to match the polymer production rate, comonomer conversion, and polymer M_n for several parallel and series grades. Next, we deconvolute the measured polymer molecular weight distribution into a number of Flory distributions. In the third step, we use the deconvolution results to expand the single-site kinetics to multisite kinetics. We adjust the kinetic parameters in the multisite model to fit the polymer production rate, comonomer conversion, M_n, and PDI of the polymer for several parallel and series grades.

In the available plant data, the polymerization reactors are at approximately the same temperature. We therefore do not consider the effect of temperature on the polymerization kinetics.

3.2. Homopolymerization Kinetic Scheme. We develop a Ziegler−Natta reaction subset to describe the observed phenomena and match targets for several grades in the HDPE slurry process. Table 11 lists the homopolymerization reactions that we consider. We describe these reactions in the following sections.

3.2.1. Catalyst Activation. In Ziegler−Natta systems, an aluminum alkyl cocatalyst, such as triethyl aluminum, is typically used to activate the sites on the catalyst. The cocatalyst is believed to form a complex with the catalyst sites that makes them active for polymerization. Equation 11 shows the reaction for site activation by cocatalyst. In this reaction, the transition-metal catalyst (CAT) reacts with the co-

Table 11. Reaction Subset Used in the Ziegler−Natta Homopolymerization Kinetics

reaction number	description
1	catalyst site activation by cocatalyst
2	chain initiation
3	chain propagation
4	chain transfer to hydrogen
5	chain transfer to monomer
6	reversible catalyst site inhibition
7	spontaneous catalyst site deactivation

catalyst (COCAT) to form vacant sites ($P_{0,i}$) of type i

$$CAT_i + COCAT \xrightarrow{k_{act,i}} P_{0,i} \tag{11}$$

where $k_{act,i}$ is the rate constant for activation of site type i by cocatalyst. The vacant sites are capable of producing polymer chains by reacting with monomer during chain initiation and subsequent propagation.

Typically, Ziegler−Natta catalysts activate almost completely in several minutes, and we therefore choose a relatively high rate constant for site activation. Alternatively, we can determine the rate constants for site activation and deactivation using data for catalyst activity profiles from experiments using laboratory-scale semibatch reactors.

As typical Ziegler−Natta catalysts are heterogeneous in nature (active metal on a support), the model includes a parameter (max-sites) for the concentration of catalyst sites per unit mass of catalyst. Typical values of the max-sites parameter range from 1.0×10^{-5} to 1.0×10^{-3} mol of sites per g of catalyst. This parameter controls the sensitivity of the polymer production rate to changes in catalyst flow rate. Changing the value of this parameter proportionally scales the effects of the site-based reactions (propagation, chain transfer, etc.). We can use it to change the magnitudes of these reactions without changing their values relative to each other. Hence, it changes the polymer production rate but does not affect the polymer molecular weight averages or copolymer composition.

3.2.2. Chain Initiation. A monomer molecule reacts with a vacant site to initiate chain growth

$$P_{0,i} + M \xrightarrow{k_{ini,i}} P_{1,i} \tag{12}$$

where M is the monomer (ethylene), $P_{1,i}$ is a propagation site of type i with an attached polymer chain containing one segment, and $k_{ini,i}$ is the rate constant for chain initiation at site type i.

It is not possible to determine the rate constants for chain initiation and propagation separately, because of the limited types of data measurements that can be made. Hence, we set the rate constant for ethylene chain initiation equal to the rate constant for propagation of ethylene monomer on ethylene active segments. Similarly, we set the rate constants for comonomer chain initiation equal to the rate constants for homopropagation of these monomers.

3.2.3. Chain Propagation. The polymer chain grows rapidly by the successive addition of monomer molecules at the catalyst site

$$P_{n,i} + M \xrightarrow{k_{p,i}} P_{n+1,i} \tag{13}$$

where $P_{n,i}$ and $P_{n+1,i}$ are polymer chains of length n and $n + 1$ segments, respectively, associated with catalyst site type i and $k_{p,i}$ is the rate constant for chain propagation for site type i. In general, a linear increase in the rate constants for propagation yields a linear increase in molecular weight.

3.2.4. Chain Transfer. Chain transfer occurs when a monomer or chain-transfer agent disengages a polymer chain from the catalyst, rendering it inactive or dead, and initiates the growth of a new chain. Most slurry HDPE processes use hydrogen as a chain-transfer agent to control the molecular weight of the polymer product. For hydrogen, the reaction is

$$P_{n,i} + H_2 \xrightarrow{k_{th,i}} D_n + P_{0,i} \tag{14}$$

where D_n is a dead polymer chain of length n and $k_{th,i}$ is the rate constant for chain transfer to hydrogen for site type i.

The chain-transfer reaction to monomer is slightly different, as it produces an initiated chain instead of a vacant catalyst site

$$P_{n,i} + M \xrightarrow{k_{tm,i}} D_n + P_{1,i} \tag{15}$$

where $k_{tm,i}$ is the rate constant for chain transfer to monomer for site type i and $P_{1,i}$ is an initiated chain associated with site type i.

We adjust the rate constants for chain transfer to hydrogen and to monomer to match the molecular weight of the HDPE produced over several reactors and grades with different H_2/C_2H_4 ratios in the reactor overheads. Note that the reaction with hydrogen produces a vacant catalyst site, whereas the reaction with monomer produces an initiated catalyst site. Adjusting the rate constant for chain transfer to monomer can disrupt the equilibrium number of inhibited catalyst sites, because the rate of chain initiation competes with that of hydrogen inhibition.

3.2.5. Forward and Reverse Catalyst Inhibitions. Some species, such as hydrogen, are known to cause a decrease in the rate of polymerization in some Ziegler−Natta catalyst systems. This rate depression appears to be reversible and disappears upon removal of the hydrogen. Slurry HDPE processes typically operate with two reactors in series to make a polymer product with a bimodal MWD. They do this by making close to 50% of the total polymer in the first reactor with a low average molecular weight and 50% of the polymer in the second reactor with a high average molecular weight. The catalysts used in these processes exhibit the reaction for reversible site inhibition by hydrogen, and incorporation of this effect is essential for modeling the production rates in each reactor of the series configuration. We use forward and reverse catalyst inhibitions by hydrogen to represent this behavior. The forward reaction is

$$CAT_i + xH_2 \xrightarrow{k_{finh,i}} ICAT_i \tag{16}$$

where $k_{finh,i}$ is the rate constant for forward inhibition of catalyst of site type i. The reverse reaction is

$$ICAT_i \xrightarrow{k_{rinh,i}} CAT_i + xH_2 \tag{17}$$

where $k_{rinh,i}$ is the rate constant for reverse inhibition of site type i. We adjust these rate constants to match

the production rate of HDPE in each reactor in the series configurations.

3.2.6. Spontaneous Catalyst Deactivation. The active sites on the catalyst can undergo spontaneous deactivation to form dead sites that are no longer active

$$P_{0,i} \xrightarrow{k_{d,i}} CAT_i \tag{18}$$

where $k_{d,i}$ is the rate constant for spontaneous catalyst deactivation for site type i. Increasing this rate constant decreases the production rate of HDPE. Also, if the chain-transfer rates are low, catalyst deactivation can affect the number-average molecular weight.

3.3. Copolymerization Kinetic Scheme. Comonomers are commonly used to produce HDPE products of varying densities. The introduction of α-olefins, such as propylene, 1-butene, and 1-hexene, creates short-chain branching along the polymer backbone, lowering the crystallinity of the polymer.

We assume that the rate of propagation of a monomer (or comonomer) depends only on the active segment (last monomer added to the chain) and the propagating monomer. This is commonly referred to as the terminal model for copolymerization kinetics. For a system with two monomers, we expand the propagation reactions as follows

$$P^1_{n,i} + M_1 \xrightarrow{k^{11}_{p,i}} P^1_{n+1,i} \tag{19}$$

$$P^1_{n,i} + M_2 \xrightarrow{k^{12}_{p,i}} P^2_{n+1,i} \tag{20}$$

$$P^2_{n,i} + M_1 \xrightarrow{k^{21}_{p,i}} P^1_{n+1,i} \tag{21}$$

$$P^2_{n,i} + M_2 \xrightarrow{k^{22}_{p,i}} P^2_{n+1,i} \tag{22}$$

where $P^j_{n,i}$ is a polymer chain of length n, associated with site type i, that has an active segment corresponding to monomer of type j and $k^{jk}_{p,i}$ is the rate constant for propagation, associated with site type i, for a monomer of type k adding to a chain with an active segment of type j.

For HDPE, the concentration of comonomer segments in the polymer and the concentration of comonomer active segments (i.e., segments attached to an active site) are small. Hence, the homopropagation reaction for ethylene is the primary factor responsible for ethylene conversion, whereas the propagation reaction for comonomer adding to a chain ending with an ethylene active segment dominates the consumption of comonomer. The concentration of ethylene active segments is very high relative to that of comonomer active segments. As a result, the propagation reactions involving comonomer active segments provide only minor contributions to the conversion of monomer and comonomer, as well as the HDPE production rate.

We expand the reactions for chain initiation and chain transfer to both monomer and hydrogen in a similar fashion, to consider the reaction of these species with the different monomers/active segments on the polymer chains. For chain initiation

$$P_{0,i} + M_j \xrightarrow{k^j_{ini,i}} P^j_{1,i} \tag{23}$$

where M_j is a monomer of type j and $k^j_{ini,i}$ is the rate of chain initiation for monomer j at site type i.

For chain transfer to hydrogen

$$P^j_{n,i} + H_2 \xrightarrow{k^j_{th,i}} D_n + P_{0,i} \tag{24}$$

where $k^j_{th,i}$ is the rate constant for chain transfer to hydrogen associated with a chain ending with a monomer unit of type j at site type i. Similarly, we have the copolymerization reactions for chain transfer to monomer

$$P^j_{n,i} + M_k \xrightarrow{k^{jk}_{tm,i}} D_n + P^k_{1,i} \tag{25}$$

where $k^{jk}_{tm,i}$ is the rate constant for chain transfer for a monomer of type k reacting with a growing chain ending in a monomer unit of type j at site type i.

3.4. Oligomer Production. Slurry HDPE processes produce oligomer, which is a low-molecular-weight polymer species that dissolves in the hexane diluent. Using plant data for the molecular weight of the oligomer, we model its production by reacting stoichiometric amounts of ethylene and hydrogen

$$xC_2H_4 + H_2 \rightarrow \text{oligomer} \tag{26}$$

where x represents the number of ethylene segments in the oligomer. Because we know the amount of oligomer produced, we adjust the extent of this reaction in the model to match the oligomer production rate. Specifically, the extent of reaction represents the changes in the number of moles of ethylene due to reaction divided by the stoichiometric coefficient x.

3.5. Determination of Kinetic Parameters. 3.5.1. Introduction. Here, we provide a general methodology for simultaneously fitting the kinetic parameters to plant data for multiple product grades. The fine-tuning of kinetic parameters to match plant data can be a difficult task. Adjustment of the rate constant for each reaction can affect several simulation variables simultaneously. The methodology assumes no information about the kinetic activity of the catalyst or the number of catalyst sites per mass of catalyst.

As mentioned previously, we do not consider temperature effects on the polymerization kinetics, as all of the reactors in the plant were operated at about the same temperature. Because the polymerization reactions are highly coupled, the determination of temperature dependence for each individual reaction would require extensive experimentation. Moreover, few data are available in the open literature for the temperature dependence of the reactions for Ziegler−Natta systems.

We divide the procedure into two parts. In the first part, we assume that the catalyst contains a single site type. This simplification permits us to model accurately only the M_n, not the M_w or the PDI. We adjust the kinetic parameters to match the HDPE production rate in each reactor and the conversions of monomer and comonomer, in addition to the HDPE M_n.

The second part of the procedure involves the introduction of multiple catalyst site types. We deconvolute the MWD for the polymer product into distributions for each site type. This procedure gives the minimum number of site types allowing for the accurate computation of the polymer MWD, as well as the relative rate of propagation and the polymer M_n produced by each

Table 12. Simulation Targets for the Models for Catalysts with Single and Multiple Site Types

model for single-site catalyst	model for multiple-site catalyst
HDPE production in each reactor	HDPE production in each reactor
monomer and comonomer conversions	monomer and comonomer conversions
HDPE M_n	HDPE M_n
	relative production of HDPE by each site type
	M_n of HDPE at each site type
	fraction of inhibited catalyst sites
	HDPE PDI

site type. The simulation targets include those for the single-site model, as well as the relative amount of polymer produced at each site type, the M_n for HDPE for each site type, the fraction of inhibited catalyst sites as determined in the single-site model, and the PDI of the HDPE product. Table 12 summarizes the simulation targets for the single-site and multisite models.

Section 3.5.2 describes the determination of the kinetic parameters for the single-site model. We manually iterate between each of the polymer grades until we obtain a set of kinetic parameters that satisfies the simulation targets for each one (Table 12). Section 3.5.3 explains the procedure for deconvoluting the MWD of the HDPE to determine the number of catalyst site types and the kinetic behavior for each site. Section 3.5.4 details the methodology for using the multisite model to adjust the kinetic parameters simultaneously to match all of the simulation targets given in Table 12.

3.5.2. Single-Site Kinetic Model. We begin by modeling the catalyst as containing a single site type. Assuming a single-site catalyst, we can accurately model all of the reaction phenomena except the polymer PDI. The motivation for using this approach is that the consideration of a multisite catalyst significantly increases the number of kinetic parameters that we must determine, because of the increase in the number of reactions involving catalyst sites. The number of reactions can exceed 60, depending on the number of site types used. The parameter determination is much simpler using a two-step method than trying to establish all of the parameter values at once.

We establish a base set of kinetic parameters using sources in the open literature. Table 13 gives their values. We also use an initial concentration of active catalyst sites on the catalyst species of 0.0002 mol of sites/mol of Ti.[20] We use these numbers as initial values in the model and then apply an iterative methodology to adjust them to match model predictions with plant data.

Figure 14 shows the methodology we use to determine the kinetic parameters for the single-site model to match plant data for multiple product grades (both parallel and series configurations). We step through the algorithm manually. Using the base set of kinetic parameters in Table 13, we first adjust the concentration of active sites on the catalyst species. Only a fraction of the transition-metal sites of the catalyst are available for polymerization. Increasing the active-site concentration on the catalyst increases the rates of reaction involving catalyst, such as activation, chain initiation, and chain propagation, while maintaining the relative ratios between them. Thus, we can increase the production rate of the HDPE while maintaining its comonomer composition and number-average molecular weight.

We adjust the rate constants for chain propagation to match the conversions of monomer and comonomer. The primary reactions affecting monomer and comonomer conversions are those for monomer−monomer and monomer−comonomer propagations, respectively, due to the high monomer concentration relative to that of comonomer. Chain propagation also affects the molecular weight. Adjusting the rate constant for chain transfer to monomer affects the number-average molecular weight of the HDPE, especially when the concentration of chain-transfer agent is low.

Table 13. Base Set of Kinetic Parameters for the Single-Site Model[a]

reaction	reactant 1	reactant 2	k[b]	ref	comments
cat-act	catalyst	cocatalyst	1	17	
chain-ini	catalyst	ethylene	14.6		*c*
chain-ini	catalyst	propylene	9.8		*c*
chain-ini	catalyst	1-butene	9.8		*d*
propagation	ethylene	ethylene	14.6	18	
propagation	ethylene	propylene	0.81	18	
propagation	propylene	ethylene	41	18	
propagation	propylene	propylene	9.8	18	
propagation	ethylene	1-butene	0.81		*d*
propagation	1-butene	ethylene	41		*d*
propagation	1-butene	1-butene	9.8		*d*
chat-agent	ethylene	hydrogen	0.088	17	
chat-agent	propylene	hydrogen	0.088	17	
chat-agent	1-butene	hydrogen	0.088		*d*
chat-mon	ethylene	ethylene	0.0021	17	
chat-mon	ethylene	propylene	0.006		*e*
chat-mon	propylene	ethylene	0.0021		*e*
chat-mon	propylene	propylene	0.006		*e*
chat-mon	ethylene	1-butene	0.006	17	
chat-mon	1-butene	ethylene	0.0021	17	
chat-mon	1-butene	1-butene	0.006	17	
fwd site inh	catalyst	hydrogen	2000	17	
rev site inh	catalyst		0.0003	17	
spon-deact	catalyst		0.0001	17	

[a] We do not consider temperature effects on the polymerization kinetics, and we therefore do not take activation energies into account. [b] General units are L/mol·s. [c] Assumed to be equal to that for homopropagation. [d] Assumed to be equal to the analogous rate constant involving propylene. [e] Assumed to be equal to the analogous rate constant involving 1-butene.

For the series grades, we adjust the rate constants for forward and reverse catalyst inhibitions by hydrogen. Note that the series reactors operate at the same temperature. In general, increasing the rate constant for forward site inhibition decreases the polymer production rate in the first reactor while increasing the production rate in the second reactor. Increasing the rate constant for reverse inhibition affects the relative production rates in the two reactors simultaneously, so we can use it to adjust the HDPE production rates in the two reactors while maintaining the same ratio of production in each one.

We iterate between all of the product grades until we obtain a set of single-site kinetic parameters that allows the model to match the plant data (except the PDI) for each grade. The next section describes the use of gel permeation chromatography (GPC) for obtaining the MWD of the polymer and a quantification of the multisite behavior of the catalyst.

3.5.3. Deconvolution of Molecular Weight Distribution Data. We can apply a statistical algorithm

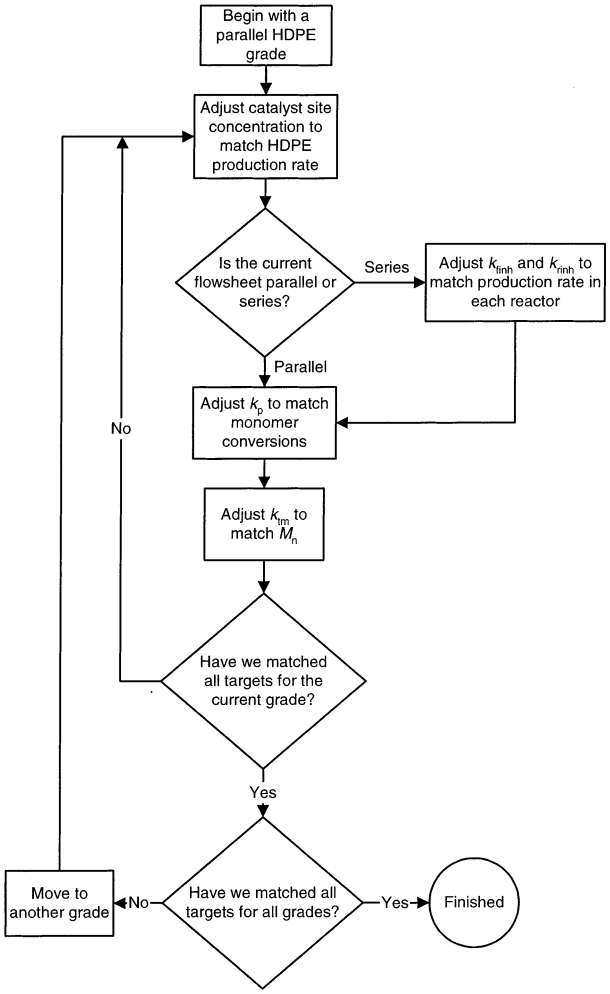

Figure 14. Methodology for simultaneously determining the kinetic parameters for a single-site catalyst to match plant data for multiple HDPE grades.

to deconvolute the polymer MWD to determine a most-probable chain-length distribution for each of a determined number of catalyst site types. The methodology presented by Soares and Hamielec[4] allows one to determine the minimum number of catalyst site types that gives an accurate representation of the molecular weight distributions generated by Ziegler−Natta catalysts, as well as the weight fraction and number-average molecular weight of polymer produced by each site type. The consideration of these site types, each with its respective reactivity, enables us to model the broad molecular weight distribution of the HDPE accurately.

Soares and Hamielec use the following expression to represent the most-probable weight chain-length distribution produced by each site type

$$w_i(n) = \tau_i^2 n \exp(-\tau_i n) \tag{27}$$

Here, $w_i(n)$ is the weight fraction of polymer of chain length n produced by site type i. τ_i is a fitting parameter for site type i and represents the inverse of the M_n of polymer produced at that site. The weight chain-length distribution of the entire polymer is a weighted sum of the distributions produced by each site type. The weighting factor is the mass fraction of polymer

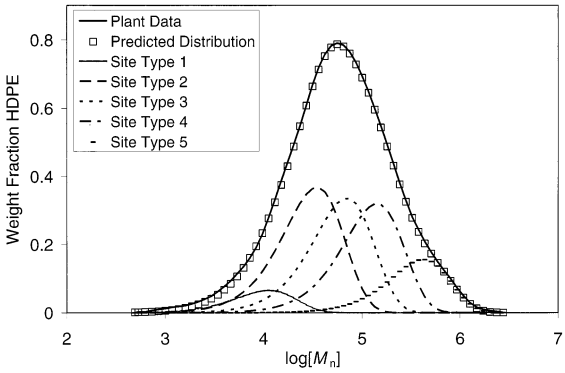

Figure 15. GPC deconvolution results for a representative HDPE sample from the parallel reactor configuration. Five catalyst site types accurately describe the experimental molecular weight distribution.

Table 14. Deconvolution Results for a Representative Sample of HDPE Produced in the Parallel Process

site type	HDPE weight fraction, m_i	τ_i (M_n^{-1})	τ_i^{-1} (M_n)
1	0.0529	1.76×10^{-4}	5.69×10^{3}
2	0.295 38	5.75×10^{-5}	1.74×10^{4}
3	0.269 79	2.85×10^{-5}	3.50×10^{4}
4	0.256 85	1.41×10^{-5}	7.08×10^{4}
5	0.125 04	4.76×10^{-6}	2.10×10^{5}

produced at each site type. The expression for the total polymer is

$$W(n) = \sum_{i=1}^{j} m_i w_i(n) \tag{28}$$

where $W(n)$ is the weight fraction of polymer of chain length n, m_i is the mass fraction of polymer produced at site type i, and j is the total number of site types.

We use software produced by Polythink Inc.[21] to deconvolute the GPC data for HDPE. It incorporates the methodology presented by Soares and Hamielec. The program determines the minimum number of site types that accurately describes the MWD, the weight fraction of polymer and corresponding M_n produced at each site type, and the predicted M_n and M_w for the entire distribution.

Table 14 shows a representative set of deconvolution results for the parallel rector configuration. Figure 15 illustrates the MWD predicted for each site type, as well as a comparison of the prediction of the overall MWD with the experimental curve. The results indicate that a five-site model can describe the molecular weight distribution of this particular sample. In the next section, we show how to use these results to determine kinetic parameters for a reaction set considering multiple catalyst site types.

3.5.4. Multisite Kinetic Model. Once we establish a set of single-site kinetic parameters that allows the model to match the simulation targets for each grade (see Table 12), we introduce multiple site types, the exact number of which is determined by the GPC deconvolution method described in the previous section. It is important to note that the MWD from the second reactor in the series process is not useful for determining kinetic parameters for the site types. The polymer exiting this reactor results from reaction phenomena occurring in the two reactors, and there is no reasonable way to decouple these events for the purpose of establishing kinetic parameters for individual reactions.

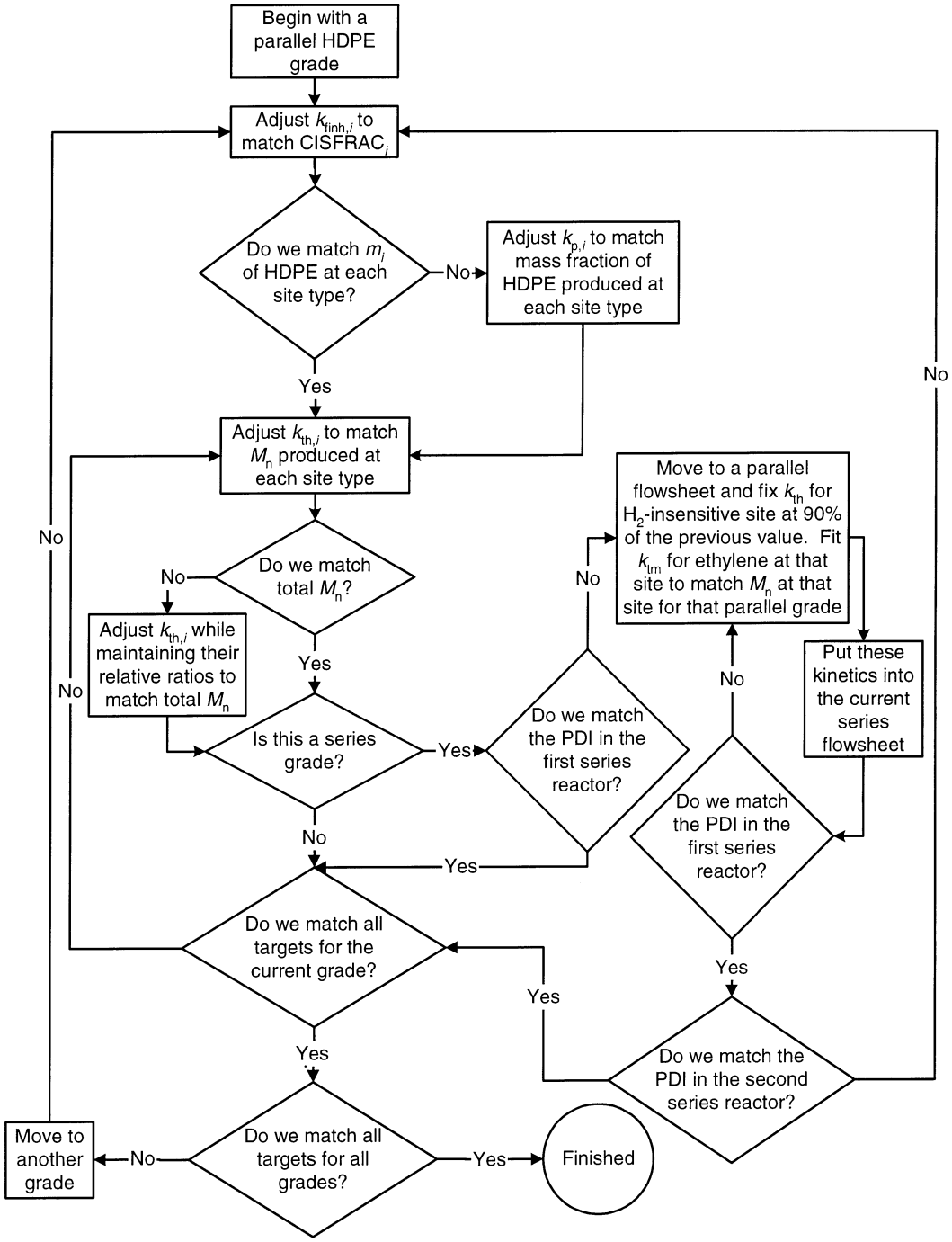

Figure 16. Methodology for simultaneously determining the kinetic parameters for a catalyst with multiple site types to match plant data for several HDPE grades.

The transition from the single-site to multisite catalyst introduces three new criteria for determining the kinetic parameters. These are the weight fraction and M_n of polymer produced at each site type and the fraction of inhibited catalyst sites. The first two targets result from the MWD deconvolution described in the previous section. The fraction of inhibited sites affects the production rate of polymer, and one must maintain the fraction that results from the single-site modeling step to preserve the correct relative amounts of polymer produced in each reactor for the series grades.

We multiply the rate constant for propagation determined in the single-site model by the weight fraction of polymer produced at site type i, m_i, (see Table 14) to obtain the initial values for each propagation rate constant

$$k_{p,i}^{ij} = n_{st} k_p^{ij} m_i \tag{29}$$

where n_{st} is the number of site types considered in the model. We must multiply the rate constants by n_{st} (5, in our case) because the concentration of total sites is n_{st} times that of the individual sites. Note that we assume the catalyst contains an equal number of moles of each site type. We adjust the rate constants for chain transfer to hydrogen and to monomer to match the number-average molecular weight produced at each site type.

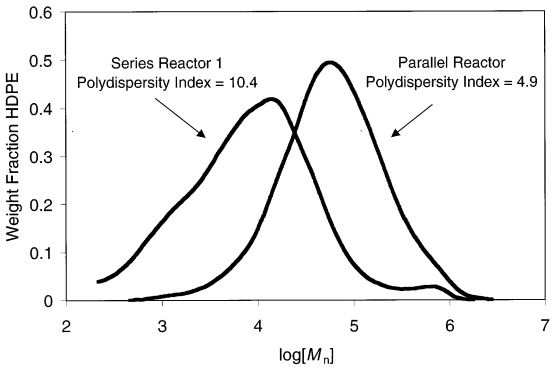

Figure 17. Comparison of MWDs for two different grades of HDPE. We hypothesize that the Ziegler−Natta site type producing high-molecular-weight polymer is insensitive to hydrogen concentration.

The single-site model yields an equilibrium mole fraction of inhibited catalyst sites. We denote this value as $CISFRAC_{ss}$, where

$$CISFRAC_{ss} = \frac{\text{number of moles of inhibited catalyst sites}}{\text{total number of moles of catalyst sites}} \quad (30)$$

One must maintain this total fraction in the multisite model to preserve the polymer properties computed in the single-site model. We represent the corresponding targets in the multisite model, $CISFRAC_i$, as the quotient of the single-site value and the number of site types

$$CISFRAC_i = \frac{\text{number of moles of inhibited sites of type } i}{\text{total number of moles of all site types}} = \frac{CISFRAC_{ss}}{n_{st}} \quad (31)$$

Figure 16 shows the iterative scheme for determining kinetic parameters in the multisite model. It is more complex than that for the single-site model because of the additional simulation targets. As with the single-site model, we step through the algorithm manually. Beginning iterations with a parallel model, we adjust the rate constants for forward site inhibition to match the inhibited fraction for each site type. If the mass fraction of polymer produced at each site does not match the target values determined from deconvolution, we adjust the rate constants for propagation. We then adjust the rate constants for chain transfer to hydrogen to match the number-average molecular weights at each site type. If the number-average molecular weight of the total polymer is not correct, we adjust the rate constants for chain transfer to hydrogen for each catalyst site type while maintaining their relative values.

For the series grades, we check the PDI produced in each reactor. If, at this point, the kinetic parameters do not give a match for the PDIs in the first reactors for all grades, we hypothesize that at least one of the site types is insensitive to a reactant involving chain transfer, such as hydrogen. We illustrate this approach using MWDs for representative HDPE. Figure 17 compares the MWDs for HDPE produced in reactors that have different hydrogen concentrations. In this case, the series reactor has a higher hydrogen concentration than the parallel reactor. Because hydrogen limits the molecular weight of the polymer, we expect to see the entire molecular weight distribution shift horizontally to the left as the hydrogen concentration increases. However, if a site type is insensitive to the hydrogen concentration, a shift does not occur. This is consistent with the behavior appearing in Figure 17.

Table 15. Simulation Targets for Each Polymer Grade and the Corresponding Adjusted Model Parameters

simulation targets	adjusted parameters
monomer conversions (HDPE production rate)	propagation rate constants for monomer and comonomer
HDPE PDI	relative propagation rate constant for each site type, determined using deconvolution of MWD
mass fraction of polymer produced at each site type	propagation rate constants for individual site types
M_n produced by each site type	chain-transfer rate constants for individual site types

In accordance with this observation, we include steps in the methodology to allow the kinetic model to match the PDI for grades of varying hydrogen concentration. We return to the previous fitted grade in the algorithm, preferably a parallel model. We reduce the rate of chain transfer to hydrogen by 10% for the insensitive site while increasing the rate of chain transfer to monomer to refit the number-average molecular weight produced at that site. We then place these adjusted kinetic parameters back into the model for the current grade and check the PDI. We repeat this loop until we match the PDI in the first reactor for each grade. We then check the PDI for the second series reactors and return to the beginning of the algorithm for that grade if it does not match. We repeat this process until we match the data for each reactor in each grade.

Table 15 summarizes the model parameters that we adjust to match the primary targets for the plant data. In the next section, we compare model predictions to data for eight HDPE grades.

4. Simulation Results

4.1. Steady-State Model Validation. We validate the model using plant data from four parallel and four series grades of HDPE, produced in two large-scale commercial plants (144 000 and 240 000 tons/year). Differences between the processes for each grade include reactor configurations (parallel and series), feed rates for raw materials, and unit-operation conditions. Because we used these same data when developing the kinetic parameters, we can expect that accurate prediction by our model is generally limited to similar process conditions. The utilization of plant data at varying reactor temperatures, for example, would permit the consideration of activation energies in the kinetic expressions, resulting in an expansion of the predictive capabilities of the model.

Figures 18−20 compare the model predictions with data from plant A for the HDPE produced in each reactor. The model accurately predicts the production rate, M_n, and PDI for each grade. The PDI predictions reflect the validity of the kinetic modeling and parameter determination for the multisite catalyst.

Figures 21 and 22 show model validations for the vapor flow in the reactor overhead and the reactor residence time, respectively, for plant A. The process model provides good agreement with each of these process variables. Accurate prediction of the volumetric

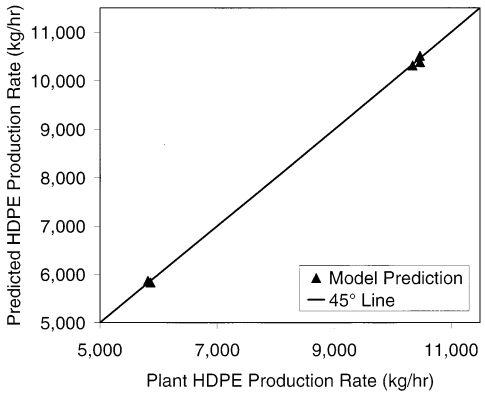

Figure 18. Comparison of model predictions with plant data for HDPE production rate.

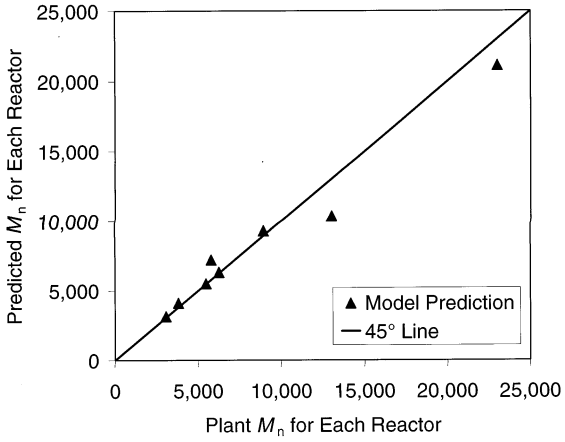

Figure 19. Comparison of model predictions with plant data for the number-average molecular weight of HDPE for each reactor.

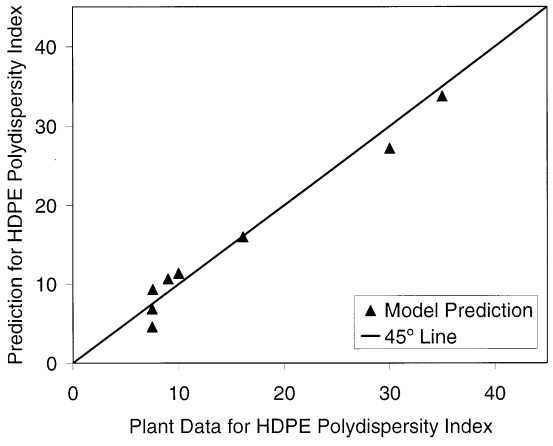

Figure 20. Comparison of model predictions with plant data for the HDPE polydispersity index.

flow in the vapor overhead is important because of limitations in equipment capacity. The reactor residence time must be accurate because it affects all of the polymer properties.

Tables 16 and 17 compare model predictions with data from plant B.[22] The model provides good agreement with polymer properties and process variables in both the parallel and series configurations.

Here, we have presented results for a single reactor section for each of the parallel processes (refer to Figure 2). Although each parallel process essentially contains two identical process sections that receive the same fresh feeds and operate at the same conditions, identical

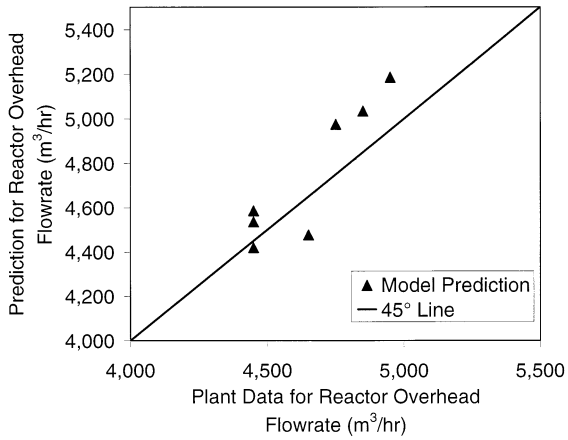

Figure 21. Comparison of model predictions with plant data for the vapor flow rate in the reactor overhead.

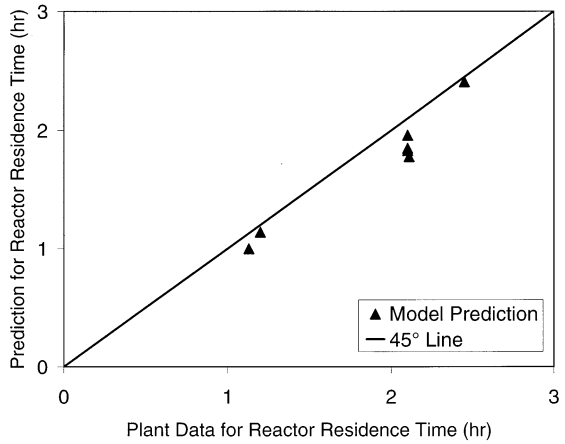

Figure 22. Comparison of model predictions with plant data for reactor residence time.

Table 16. Comparison of Model Predictions with Data for a Parallel Grade for Plant B

	plant data	model prediction
HDPE production rate (kg/h)	5096−5148	5187
ethylene conversion (%)	98−99	99.7
propylene conversion (%)	72	75.3
HDPE M_n	14 000−16 000	15 975
HDPE PDI	9−10	9.63
reactor residence time (h)	2.2	1.98
H_2/C_2H_4 molar ratio in overhead	0.65−0.68	0.643

Table 17. Comparison of Model Predictions with Data for a Series Grade for Plant B

		plant data	model prediction
HDPE production rate (kg/h)	total	9212−9306	9151
ethylene conversion (%)	total	98−99	97.4
1-butene conversion (%)	total	89	74.8
HDPE M_n	reactor 1	−	3336
	reactor 2	7000	6537
HDPE PDI	reactor 1	−	10
	reactor 2	31−35	38.9
reactor residence time (h)	reactor 1	2.5	2.68
	reactor 2	1.13	1.17
H_2/C_2H_4 molar ratio in overhead	reactor 1	6.8−7.2	7.25
	reactor 2	0.08−0.09	0.084

industrial systems rarely behave in the same way. Therefore, when constructing a robust process model, one should consider both sections on an individual basis.

4.2. Dynamic Modeling. 4.2.1. Introduction. Whereas a steady-state model does not consider changes

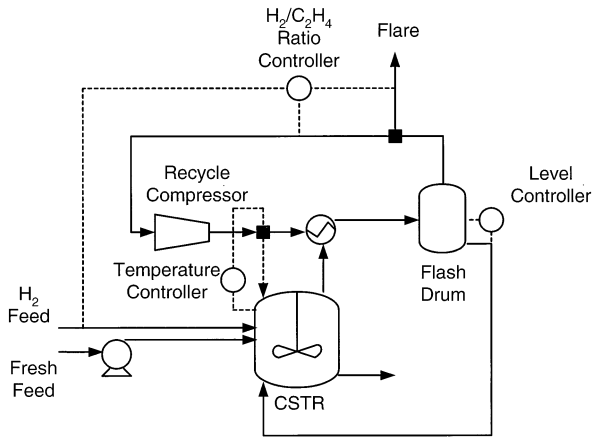

Figure 23. Simplified diagram of the control scheme for the parallel reactor configuration.

Table 18. Controlled and Manipulated Variables for the Slurry HDPE Process

controlled variables	manipulated variables
reactor temperature	overhead vapor recycle to reactor
overhead H_2/C_2H_4 molar ratio	hydrogen feed rate and overhead flare
liquid level in flash tank	liquid recycle rate to reactor

Table 19. Specifications for the Grade Change in the Parallel Configuration

	grade 1	grade 2
ethylene feed rate (kg/h)	5949	5999
propylene feed rate (kg/h)	81.7	0
overhead H_2/C_2H_4 molar ratio	0.56	1.54
catalyst feed rate (kg/h)	0.175	0.386
cocatalyst feed rate (kg/h)	0.658	0.800

in the process with time, a dynamic model permits the variation of the feed rates or vessel conditions and the tracking of the resulting process changes as they propagate through the system. A dynamic model can assist in optimizing the time required to carry out a grade change, facilitate the development of a new polymer grade, or reveal the time-dependent effects of changing a process variable. Our goal here is to demonstrate the capability and utility of a dynamic model for an industrial slurry HDPE process.

We create the dynamic process model in Aspen Dynamics by importing the corresponding steady-state model developed in Aspen Polymers Plus. We include vessel dimensions and geometries to account for the liquid levels in each unit properly.

In the following sections, we illustrate the utility of dynamic modeling by simulating a grade change for the parallel reactor configuration. Section 4.2.2 describes the control scheme for the process. Section 4.2.3 gives the feed rates and process variables for the grade change, as well as dynamic results.

4.2.2. Control Scheme. Figure 23 presents a simplified diagram illustrating the control scheme for the parallel configuration. The process includes (1) a reactor temperature controller that adjusts the amount of recycle gas returned to the reactor inlet, (2) a compositional controller that adjusts the hydrogen feed rate and the rate of recycle-gas flare to maintain a constant ratio of hydrogen to ethylene in the recycle-gas stream, and (3) a level controller in the overhead flash unit that adjusts the amount of liquid recycled to the reactor. Table 18 summarizes the controlled and manipulated variables.

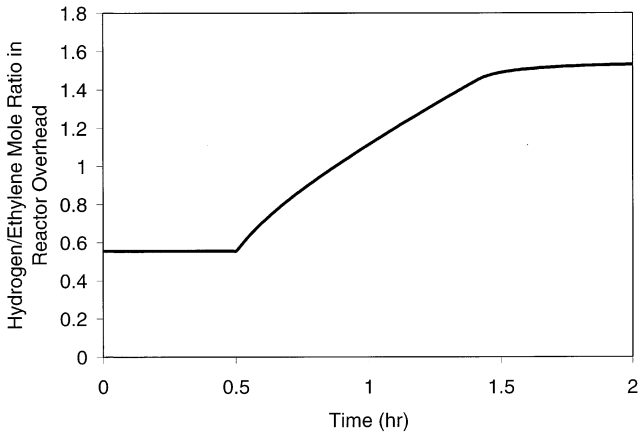

Figure 24. Change in the H_2/C_2H_4 overhead ratio during the grade change in the parallel configuration.

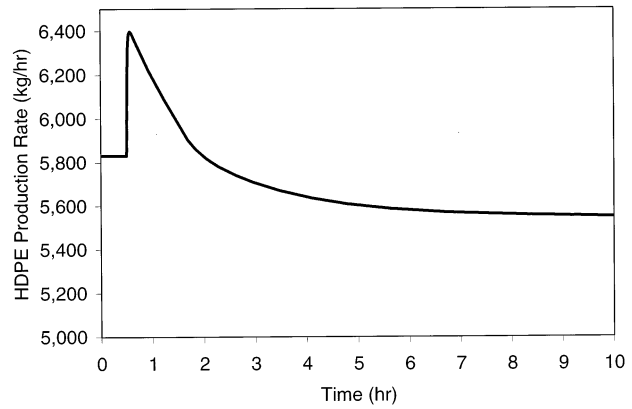

Figure 25. Effect of the grade change on the production rate of HDPE in the parallel configuration.

4.2.3. Dynamic Grade Change. Table 19 gives the key process modifications for a typical grade change for the parallel configuration. The unit-operation conditions remain the same between the two grades.

We assume an instantaneous change in the feed rates in Table 19 to the new values. We also change the set point for the H_2/C_2H_4 controller to the new value of 1.54.

Figure 24 shows the dynamic change in the H_2/C_2H_4 ratio in the reactor overhead. The controller initially increases the hydrogen feed rate to achieve the new set point. The rate at which the system reaches the new set point is mainly a function of the value for the proportional gain used for the controller. Figure 25 illustrates the effect of the grade change on the production rate of HDPE. The sharp increase is due to the increase in the catalyst feed rate. The production rate then decreases to a value below that for the first grade, because of the large increase in hydrogen concentration that results from the higher set point for the H_2/C_2H_4 ratio in the overhead. The hydrogen inhibits the catalyst, effectively reducing the concentration of active sites in the reaction mixture. Figure 26 shows the effect of the grade change on the HDPE M_n. The increase in the hydrogen and catalyst feed rates decreases the product M_n through chain transfer.

4.3. Process Retrofit. The purpose of this process retrofit is to increase the production rate of HDPE while maintaining the same product quality (i.e., polymer attributes). An increase in production requires a corresponding increase in heat removal due to polymeriza-

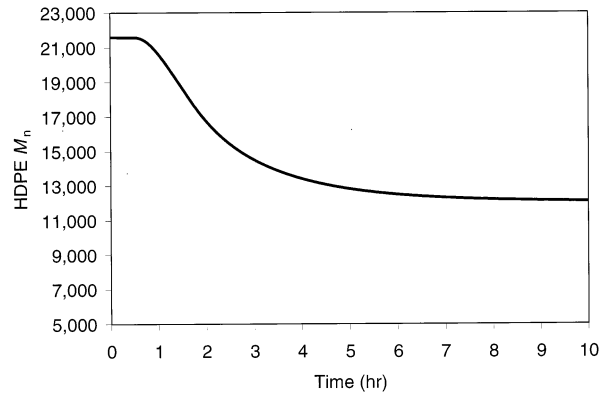

Figure 26. Effect of the grade change on the number-average molecular weight of HDPE.

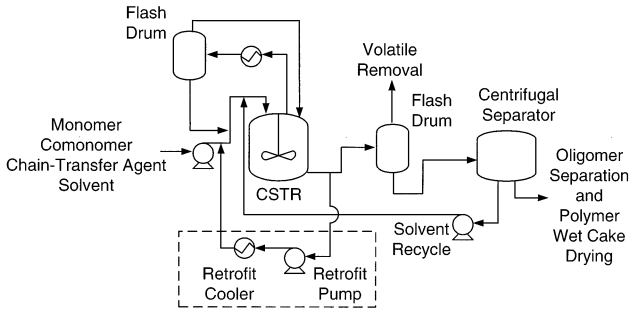

Figure 27. Flowsheet for a process retrofit applied to one reactor in the parallel configuration. Increasing the production rate increases the demands for heat removal, thereby necessitating the addition of another pump and cooler to recycle liquid to the reactor.

Table 20. Comparison of HDPE Flow Rate and Attributes for Varying Increases in Feed Rates of Raw Material for the Process Retrofit

% increase in ethylene, propylene, hexane, and mother-liquid feed rates	HDPE production rate (kg/h)	M_n	PDI	recycle gas flow rate (kg/h)	heat duty of slurry cooler (kcal/h)	slurry recycle flow rate (kg/h)
0[a]	5834	21 148	4.58	24 809	–	–
10	6426	21 093	4.58	25 622	562 108	23 244
15	6717	21 037	4.58	28 804	807 327	33 382
20	7017	20 990	4.58	28 982	1 075 000	44 459

[a] Original model.

tion. If the overhead units are already operating close to capacity, one cannot increase the rate of vapor removed from the reactor significantly to meet the additional heat-transfer requirements. We propose the addition of a pump and a heat exchanger to enable the cooling and recycling of a portion of the slurry product stream to the reactor. We use a single reactor from the parallel configuration to model the retrofit.

Figure 27 shows a flowsheet for the retrofit. We increase the feed rates of the monomer, comonomer, and solvent species by the same relative ratios to maintain the same relative concentrations of these components in the reaction mixture. This allows the properties of the polymer product to be preserved.

Table 20 summarizes the retrofit results, indicating that we can increase the production rate of HDPE by up to 20% if the overhead units can handle up to a 17% increase in the flow rate of recycle gas. As we increase the feed rate, the HDPE production rate increases, while the molecular weight undergoes an insignificant decrease. The recycle gas flow rate increases, as does the heat duty of the slurry cooler. The slurry recycle flow rate also increases.

5. Conclusions

We have developed both steady-state and dynamic models for a slurry HDPE process with two reactor configurations. We have validated the model using design and operating data from two large-scale commercial HDPE processes. The model uses a single set of kinetic and thermodynamic parameters to predict accurately the production rate, M_n, PDI, monomer conversion, and comonomer composition, as well as trends in these polymer properties with changes in key process variables, for both reactor configurations. We illustrate the utility of the dynamic model by simulating a grade change for the parallel reactor configuration.

The Sanchez–Lacombe EOS provides good predictions of the phase behavior of polymer mixtures. The Chao–Seader property method gives accurate descriptions of the phase behavior of mixtures of light hydrocarbons.

A GPC deconvolution algorithm developed by Soares and Hamielec[4] and implemented by Polythink Inc.[21] accurately describes the polydisperse nature of the HDPE produced using a multiple-site-type Ziegler–Natta catalyst. We describe a unimodal molecular weight distribution produced in a parallel reactor and a bimodal molecular weight distribution produced in the first reactor of a series configuration by assuming that the site type producing the longest chains is insensitive to the hydrogen concentration.

We propose a process retrofit that permits an increase in HDPE production rate of up to 20% while maintaining the same product quality, provided that the overhead units can handle up to a 17% increase in capacity, on the basis of simulation results.

Acknowledgment

We gratefully acknowledge Alliant Techsystems, Aspen Technology (particularly Jila Mahalec, Director of Worldwide University Program, and Joseph Boston, Senior Corporate Advisor and past President), China Petroleum and Chemical Corporation, China National Petroleum Corporation, Honeywell Specialty Materials, and Honeywell International Foundation for supporting the computer-aided design educational program at Virginia Tech. We also thank Costas P. Bokis for his assistance in this work.

Symbols

English Symbols

C_i = constant for ideal-gas heat capacity correlation (i = 1,2)
C_p^{ig} = ideal-gas heat capacity (kJ/kmol·K)
C_2H_4 = ethylene
CAT_i = inactive catalyst
$CISFRAC_i$ = fraction of catalyst site type i that is inhibited
$CISFRAC_{ss}$ = fraction of catalyst sites that are inhibited in the single-site model
COCAT = cocatalyst
CSTR = continuous stirred-tank reactor
D_n = inactive polymer chain containing n segments

$[D_n]$ = concentration of inactive polymer chains containing n segments (mol/L)
EOS = equation of state
GPC = gel permeation chromatography
H_2 = hydrogen
HDPE = high-density polyethylene
$ICAT_i$ = inhibited catalyst of site type i
k = rate constant (L/mol·s)
k_0 = preexponential factor for the rate constant
$k_{act,i}$ = rate constant for activation of catalyst site type i
$k_{finh,i}$ = rate constant for forward hydrogen inhibition of catalyst site type i
k_{ij} = binary interaction parameter for Sanchez−Lacombe equation of state
$k_{ini,i}$ = rate constant for chain initiation for catalyst site type i
$k^j_{ini,i}$ = rate constant for chain initiation of catalyst site type i by monomer j
k_p = rate constant for chain propagation for the single-site model
$k_{p,i}$ = rate constant for chain propagation for catalyst site type i
$k^{jk}_{p,i}$ = rate constant for chain propagation for monomer j adding to segment type k at catalyst site type i
$k_{rinh,i}$ = rate constant for reverse hydrogen inhibition of catalyst site type i
$k_{th,i}$ = rate constant for chain transfer to hydrogen for catalyst site type i
$k^j_{th,i}$ = rate constant for chain transfer to hydrogen for chain ending in segment type j on catalyst site type i
$k_{tm,i}$ = rate constant for chain transfer to monomer for catalyst site type i
$k^{jk}_{tm,i}$ = rate constant for chain transfer to monomer j for chain ending in segment type k on catalyst site type i
M = monomer species
m_i = mass fraction of polymer produced at catalyst site type i
M_i = monomer species of type i
M_n = number-average molecular weight
M_w = weight-average molecular weight
MWD = molecular weight distribution
n = number of monomer segments in a polymer chain
n_{st} = number of catalyst site types
P = pressure (bar)
$\bar{P}$ = reduced pressure in the Sanchez−Lacombe equation of state
P^* = pressure scale factor in the Sanchez−Lacombe equation of state (bar)
$P_{0,i}$ = activated catalyst site of type i
$P_{1,i}$ = initiated catalyst site of type i
PDI = polydispersity index, M_w/M_n
P_n = live polymer chain containing n segments
$[P_n]$ = concentration of live polymer chains containing n segments (mol/L)
$P_{n,i}$ = live polymer chain containing n segments attached to catalyst site type i
$P^j_{n,i}$ = live polymer chain containing n segments, ending in segment type j, attached to catalyst site type i
r = molecular parameter in the Sanchez−Lacombe equation of state
T = temperature (°C)
$\bar{T}$ = reduced temperature in the Sanchez−Lacombe equation of state
T^* = temperature scale factor in the Sanchez−Lacombe equation of state (K)
VLE = vapor−liquid equilibrium
VLLE = vapor−liquid−liquid equilibrium
$w_i(n)$ = weight fraction of chains of length n produced at catalyst site type i
$W(n)$ = total weight fraction of chains containing n segments
x = stoichiometric coefficient
ΔH = molar enthalpy change

Greek Symbols

η_{ij} = binary interaction parameter for Sanchez−Lacombe equation of state
λ_i = ith moment for bulk (live and dead) polymer chains
μ_i = ith moment for live polymer chains
$\nu_i^{(0)}$ = parameter in Chao−Seader fugacity coefficient model
$\nu_i^{(1)}$ = parameter in Chao−Seader fugacity coefficient model
ρ = density (kg/m^3)
$\bar{\rho}$ = reduced density in the Sanchez−Lacombe equation of state
ρ^* = density scale factor in the Sanchez−Lacombe equation of state (kg/m^3)
τ_i = adjustable parameter for chain-length distribution function
ϕ_i^{liq} = liquid fugacity coefficient of species i
ω_i = acentric factor for species i

Literature Cited

(1) Scheirs, J.; Evens, G. Polyethylene (High-Density Preparation). In *Polymeric Materials Encyclopedia*; Salamone, J. C., Ed.; CRC Press: Boca Raton, FL, 1996; p 5965.

(2) Xie, T.; McAuley, K. B.; Hsu, J. C. C.; Bacon, D. W. Gas-Phase Ethylene Polymerization: Production Processes, Polymer Properties, and Reactor Modeling. *Ind. Eng. Chem. Res.* **1994**, *33*, 449.

(3) Peacock, A. J. *Handbook of Polyethylene: Structures, Properties, and Applications*; Marcel Dekker: New York, 2000.

(4) Soares, J. B. P.; Hamielec, A. E. Deconvolution of Chain-Length Distributions of Linear Polymers Made by Multiple-Site-Type Catalysts. *Polymer* **1995**, *36*, 2257.

(5) Bokis, C. P.; Orbey, H.; Chen, C.-C. Properly Model Polymer Processes. *Chem. Eng. Prog.* **1999**, *95*, 39.

(6) Sanchez, I. C.; Lacombe, R. H. An Elementary Molecular Theory of Classical Fluids. Pure Fluids. *J. Phys. Chem.* **1976**, *80*, 2352.

(7) Lacombe, R. H.; Sanchez, I. C. Statistical Thermodynamics of Fluid Mixtures. *J. Phys. Chem.* **1976**, *80*, 2568.

(8) Sanchez, I. C.; Lacombe, R. H. Statistical Thermodynamics of Polymer Solutions. *Macromolecules* **1978**, *11*, 1145.

(9) Chao, K. C.; Seader, J. D. A General Correlation of Vapor−Liquid Equilibria in Hydrocarbon Mixtures. *AIChE J.* **1961**, *7*, 598.

(10) Reid, R. C.; Prausnitz, J. M.; Poling, B. E. *The Properties of Gases and Liquids*; McGraw-Hill: New York, 1987.

(11) Beaton, C. F.; Hewitt, G. F. *Physical Property Data for the Design Engineer*; Hemisphere Publishing Corp.: New York, 1989.

(12) Sychev, V. V.; Vasserman, A. A.; Golovsky, E. A.; Kozlov, A. D.; Spiridonov, G. A.; Tsymarny, V. A. *Thermodynamic Properties of Ethylene*; Hemisphere Publishing Corp.: New York, 1987.

(13) Gaur, U.; Wunderlich, B. Heat Capacity and Other Thermodynamic Properties of Linear Macromolecules. II. Polyethylene. *J. Phys. Chem. Ref. Data* **1981**, *10*, 119.

(14) Knapp, H.; Döring, R.; Oellrich, L.; Plöcker, U.; Prausnitz, J. M. *Vapor−Liquid Equilibria for Mixtures of Low Boiling Substances*; Chemistry Data Series; DECHEMA: Frankfurt, Germany 1982; Vol VI, Part 1.

(15) Leonard, J. Heats and Entropies of Polymerization, Ceiling Temperatures, Equilibrium Monomer Concentrations, and Polymerizability of Heterocyclic Compounds. In *Polymer Handbook*; Brandrup, J., Immergut, E. H., Grulke, E. A., Eds.; Wiley & Sons: New York, 1999; p II/363.

(16) Arriola, D. J. Modeling of Addition Polymerization Systems. Ph.D. Dissertation, University of Wisconsin, Madison, WI, 1989.

(17) McAuley, K. B.; MacGregor, J. F.; Hamielec, A. E. A Kinetic Model for Industrial Gas-Phase Ethylene Copolymerization. *AIChE J.* **1990**, *36*, 837.

(18) Cansell, F.; Siove, A.; Fontanille, M. Ethylene−Propylene Copolymerization Initiated with Solubilized Ziegler−Natta Mac-

romolecular Complexes. I. Determination of Kinetic Parameters. *J. Polym. Sci. A: Polym. Chem.* **1987**, *25*, 675.

(19) Kissin, Y. V. *Isospecific Polymerization of Olefins with Heterogeneous Ziegler−Natta Catalysts*; Springer-Verlag: New York, 1985.

(20) Nagel, E. J.; Kirillov, V. A.; Ray, W. H. Prediction of Molecular Weight Distributions for High-Density Polyolefins. *Ind. Eng. Chem. Prod. Res. Dev.* **1980**, *19*, 372.

(21) Polythink Inc., 1005 Sydenham Rd., S.W., Calgary, Alberta, Canada T2T 0T3. http://www.polythink.com (accessed August 2002).

(22) Yan, R.; Xu, X.; Khare, J.; Liu, Y. A.; Chen, C.-C. Modeling of a Commercial Slurry HDPE Process Using Polymers Plus. In *Proceedings of AspenWorld China 2000*; Aspen Technology: Cambridge, MA, 2000; p 79.

Received for review June 18, 2002
Revised manuscript received September 3, 2002
Accepted September 5, 2002

IE020451N